La mer 31: 91–101, 1993
Société franco-japonaise d'océanographie, Tokyo

Sedimentation processes in Tokyo Bay, Japan*

Tetsuo YANAGI** and Manabu SHIMIZU**

Abstract: Sedimentation patterns of riverine material in the surface sediment of Tokyo Bay have been classified into two groups, that is, fan shaped pattern such as pyrene, phosphorus, and copper and circular shaped pattern such as alkylbenzene, carbon and cadmium. Such two patterns are well reproduced by the three-dimensional numerical model experiment. Heavy and light particles are injected from three main rivers at the head of numerical model of Tokyo Bay which reproduces tidal current, residual current and density distribution of the prototype. Three-dimensional movements of injected particles due to currents, turbulence and sinking velocity are tracked by the Euler-Lagrange method including the judgment of settling of particles to the sea bottom by the critical tractive force theory. Heavy particles show the fan shaped sedimentation pattern and light particles the circular one. Calculated sedimentation patterns of riverine material are highly similar to the observed ones.

1. Introduction

It is well known that the sedimentation patterns of riverine material in surface sediment of Tokyo Bay are classified into two types. One is the fan shaped pattern in which the highest concentration is located at the mouth of rivers as shown in Fig. 1 (a). Pyrene, total phosphorus, copper, nickel and chromium take this pattern. Another is the circular shaped pattern in which the highest concentration is located at the central part of the bay as shown in Fig. 1 (b). LAS (Linear Alkyl-benzene Sulfonate), total carbon, biogenic silica, cadmium and zinc take this pattern (ISHIWA-TARI, 1988). ISHIWATARI (1988) pointed out the possibility that the riverine material which adheres to heavy particles takes the fan shaped pattern and that which adheres to light particles the circular shaped pattern.

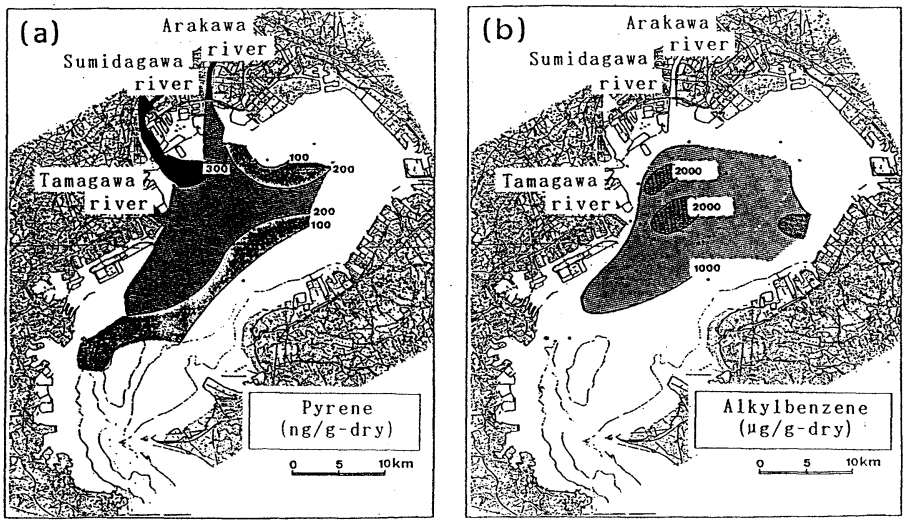

Fig. 1. Fan shaped (a) and circular shaped (b) sedimentation patterns in Tokyo bay (ISHIWATARI, 1988).

In this paper, we try to reproduce such two sedimentation patterns in Tokyo Bay with use

* Received March 19, 1993
** Department of Civil and Ocean Engineering, Ehime University Matsuyama, 790 Japan

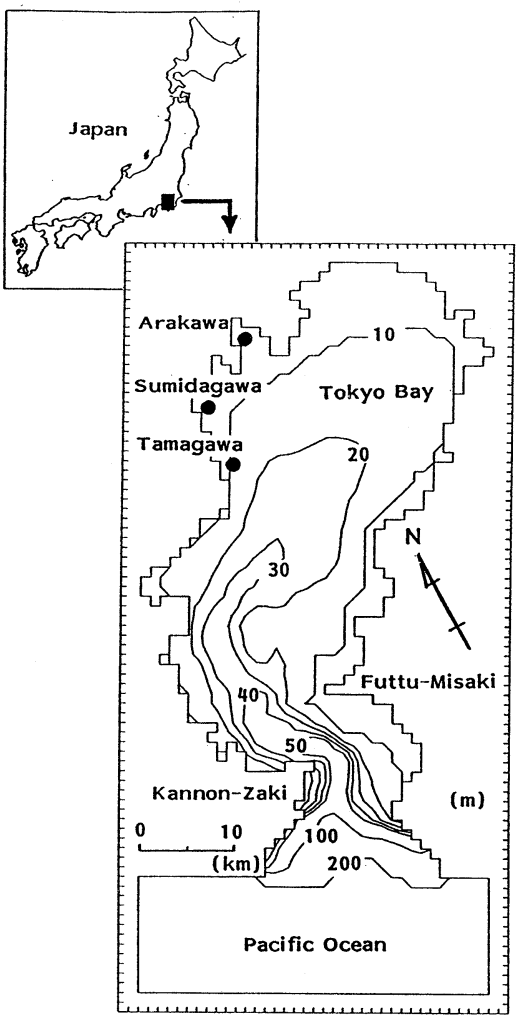

	SUMMER	WINTER
Layer 1	0 ~ 5	0 ~10
Layer 2	5 ~ 20	10 ~ 50
Layer 3	20 ~ 50	50 ~ Bottom
Layer 4	50 ~ Bottom	——

(m)

Fig. 2. Numerical model of Tokyo Bay. Full line denotes the bottom contour and the number the water depth in meter. Black circles de note the river mouths of three main rivers.

of three-dimensional numerical model by tracking the movements of heavy and light particles injected from the mouth of rivers.

2. Numerical experiment

2. 1 Currents and density fields

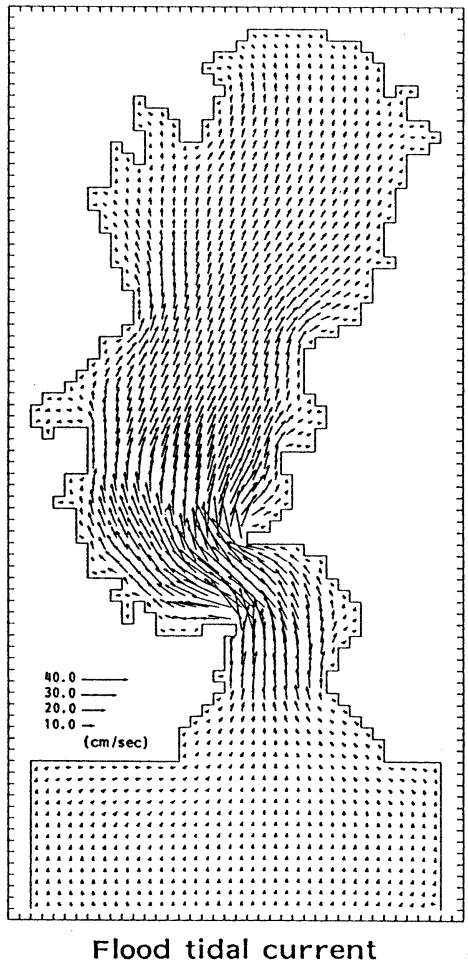

Fig. 3. Calculated maximum flood tidal current in Tokyo Bay.

The movement of riverine particless in Tokyo Bay is governed by currents, turbulence and the sinking velocity of particles. Then we first reproduce the currents of Tokyo Bay by the numerical model. Tokyo Bay is horizontally divided by the square mesh with 1 km length and the water column is vertically divided into four layers in summer and into three layers in winter as shown in Fig. 2.

The most dominant current in Tokyo Bay is the barotropic M_2 tidal current and it is well reproduced in this numerical model with use of usual method (YANAGI *et al.*, 1983). The reproduction of tide and tidal current is confirmed (YANAGI and SHIMIZU, 1991) and the calculated barotropic M_2 flood current is shown in Fig.3.

The maximum flood current of about 50 cm s^{-1} is appeared at the bay mouth and it is about 10 cm s^{-1} near the head of the bay. The ebb current flows in nearly the opposite direction with nearly the same speed. The horizontal forces due to tidal stress F_t (F_{tx}, F_{ty}) is caluculated with M_2 tidal current as follows;

$$F_{tx} = -(u\frac{\partial u}{\partial x} + v\frac{\partial u}{\partial y})$$
$$F_{ty} = -(u\frac{\partial v}{\partial x} + u\frac{\partial v}{\partial x}) \quad (1)$$

where u and v denote the x and y component of M_2 tidal current, respectively, and overbar the average over one tidal cycle. F_t is used when we caluculate the residual flow.

Next we reproduce the residual flow in Tokyo Bay which governs the longterm transport of particles and the density distribution. The density distribution of sea water affects the sinking velocity and the tractive and resistance forces of particle as shown later. Here we try to reproduce residual flows and density distributions of Tokyo Bay in summer and in winter because they are two opposite typical seasons.

The basic equations are the momentum and continuity equations under the Bussinesq and hydrostatic approximations, the advection-dispersion equations of water temperature, salinity and density and the state equation as follows;

$$\frac{\partial V}{\partial t} + (V\cdot\nabla V) + f\mathrm{k}\times V = -\frac{1}{\rho_0}\nabla P + A_h\nabla^2 V + A_v\frac{\partial^2 V}{\partial z^2} + F_t$$
$$\frac{\partial w}{\partial z} = -\nabla V \quad (3)$$
$$P = \rho_0 g\eta + \rho_0\int_{-\eta}^{z} B dz \quad (4)$$
$$B = \frac{\rho_0 - \rho}{\rho_0}\mathrm{g} \quad (5)$$
$$(\rho - 1.0)\times 10^3 = 28.14 - 0.0735\mathrm{T} - 0.00469\mathrm{T}^2 + (0.0802 - 0.002\mathrm{T})(\mathrm{S}-35) \quad (6)$$
$$\frac{\partial T}{\partial t} + V\nabla\cdot T + \mathrm{w}\frac{\partial T}{\partial z} = K_h\nabla^2 T + K_v\frac{\partial^2 T}{\partial z^2} \quad (7)$$
$$\frac{\partial S}{\partial t} + V\nabla\cdot S + \mathrm{w}\frac{\partial S}{\partial z} = K_h\nabla^2 S + K_v\frac{\partial^2 S}{\partial z^2} \quad (8)$$

where V denotes the horizontal velocity; w, vertical velocity; , horizontal differntial operator; f ($=7.8\times10^{-5}s^{-1}$), Coriolis parameter; k, vertical unit vector; ρ, density; ρ_0, overall mean density; P the pressure; T, water temperature; S, salinity; A_h ($=10^6 cm^2 s^{-1}$) and A_v; horizontal and vertical eddy visosity, respectively; g ($=980 cm\ s^{-2}$), gravitational acceleration; η, sea level height above the mean sea surface; B, the buoyancy; K_h ($=10^6 cm^2 s^{-1}$) and K_v, horizontal and vertical eddy diffusivity, respectively.

Vertical eddy viscosity and vertical eddy diffusivity are parameterized as follows,

$$A_v = K_v = 1 - 10 cm^2 s^{-1} \quad (9)$$

A_v and K_v depends on the amplitude of M_2 tidal current and it is 10 $cm^2 s^{-1}$ at bay mouth where the tidal current is the strongest and 1 $cm^2\ s^{-1}$ at the head of the bay where the tidal current is the weakest.

The boundary conditions are given on the sea surface and at the sea bottom as :

$$\frac{\partial T}{\partial z} = \frac{g\alpha Q}{\rho_0 C_p},\ \frac{\partial S}{\partial z} = 0 \ at\ z=0 \quad (10)$$
$$\frac{\partial T}{\partial t} = \rho_0 C_d |V|V,\ \frac{\partial T}{\partial z} = \frac{\partial S}{\partial z} = 0 \ at\ z=-H \quad (11)$$

where α ($=2.0\times10^{-4}$ ℃$^{-1}$) denotes the heat expan-sion coefficient; Q, heat flux through the sea surface; C_p ($=0.932$ cal g^{-1} ℃$^{-1}$), specific heat under the constant pressure; C_d ($=2.6\times10^{-3}$), the drag coefficient at the sea bottom; and H, the water depth.

The salinity efflux from rivers S is given as follows,

$$\Delta S = -SR\frac{t}{hA} \quad (12)$$

where R denotes the river discharge; S, h and A, salinity, water depth and the area of the mesh which the river flows into, t (= 400sec) the time step of calculation. Δ S is subtracted from the calculated S at the mesh which the river flows into at every time step.

The non-slip condition of velocity is given

Table 1. Different parameters in summer and in winter.

	Summer	Winter
Surface heat flux (Q)	150W/m^2	−100W/m^2
Overall mean density (ρ_0)	1.0239g/cm^3	1.0255g/cm^3
Freashwater discharge (R)		
Edogawa river	180m^3/sec	60m^3/sec
Arakawa river	90m^3/sec	30m^3/sec
Tamagawa river	90m^3/sec	30m^3/sec

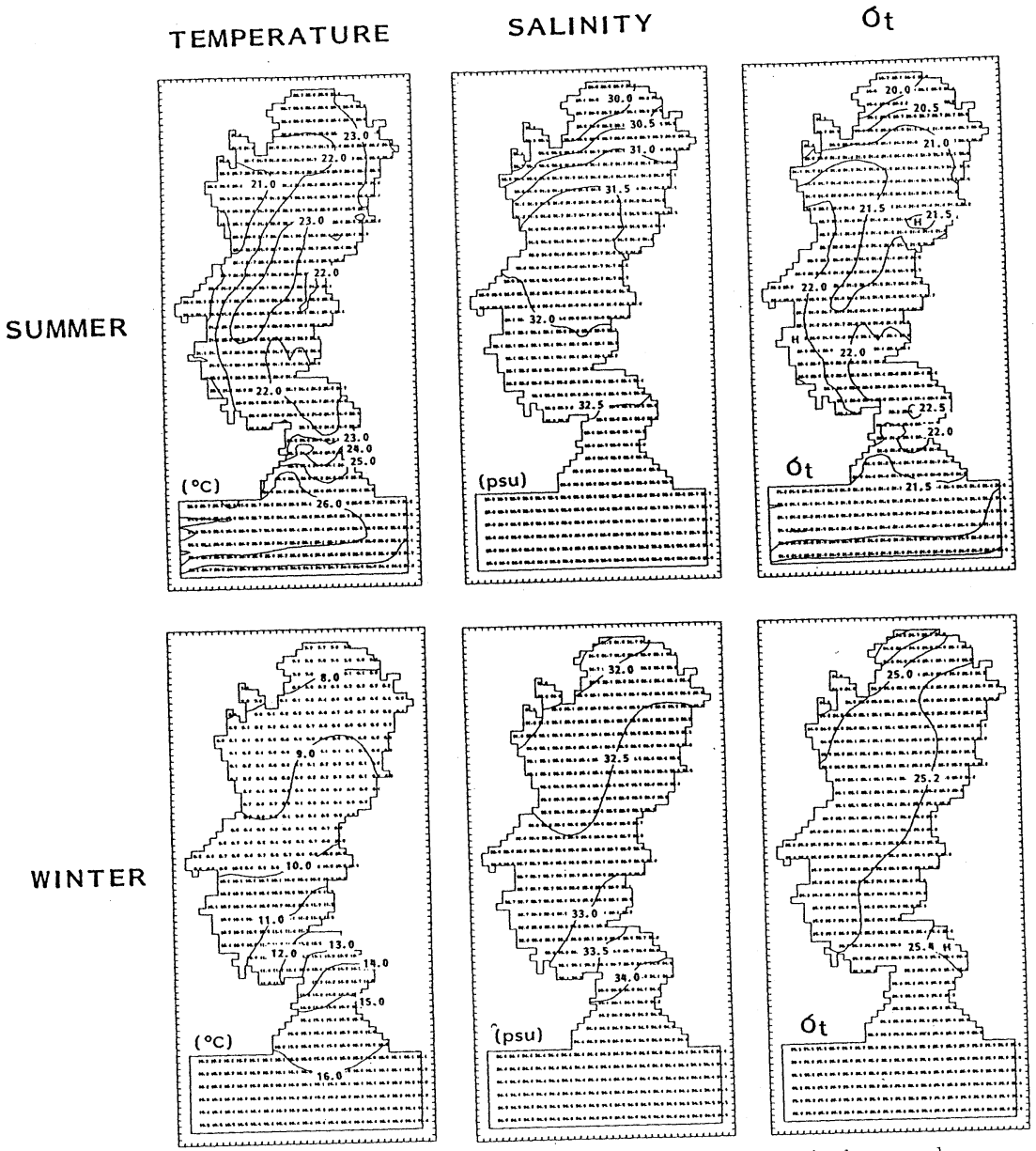

Fig. 4. Calculated water temperature, salinity and density distributions in the upper layer in summer (upper) and in winter (lower).

along the coast. The normal component of velocity to the open boundary is assumed to be zero. The horizontal gradients of water temperature and salinity across the open boundary are assumed to be zero.

Equations (1) to (12) are approximated by the finite difference and solved by the semi-implicit method (OONISHI, 1978). Different parameters in summer and winter are tabulated in Table 1.

The calculated water temperature, salinity and density distributions at the first layer in summer and in winter are shown in Fig.4. The observed water temperature, salinity and density distributions in summer and in winter (Hydrographic Office of Maritime Safety

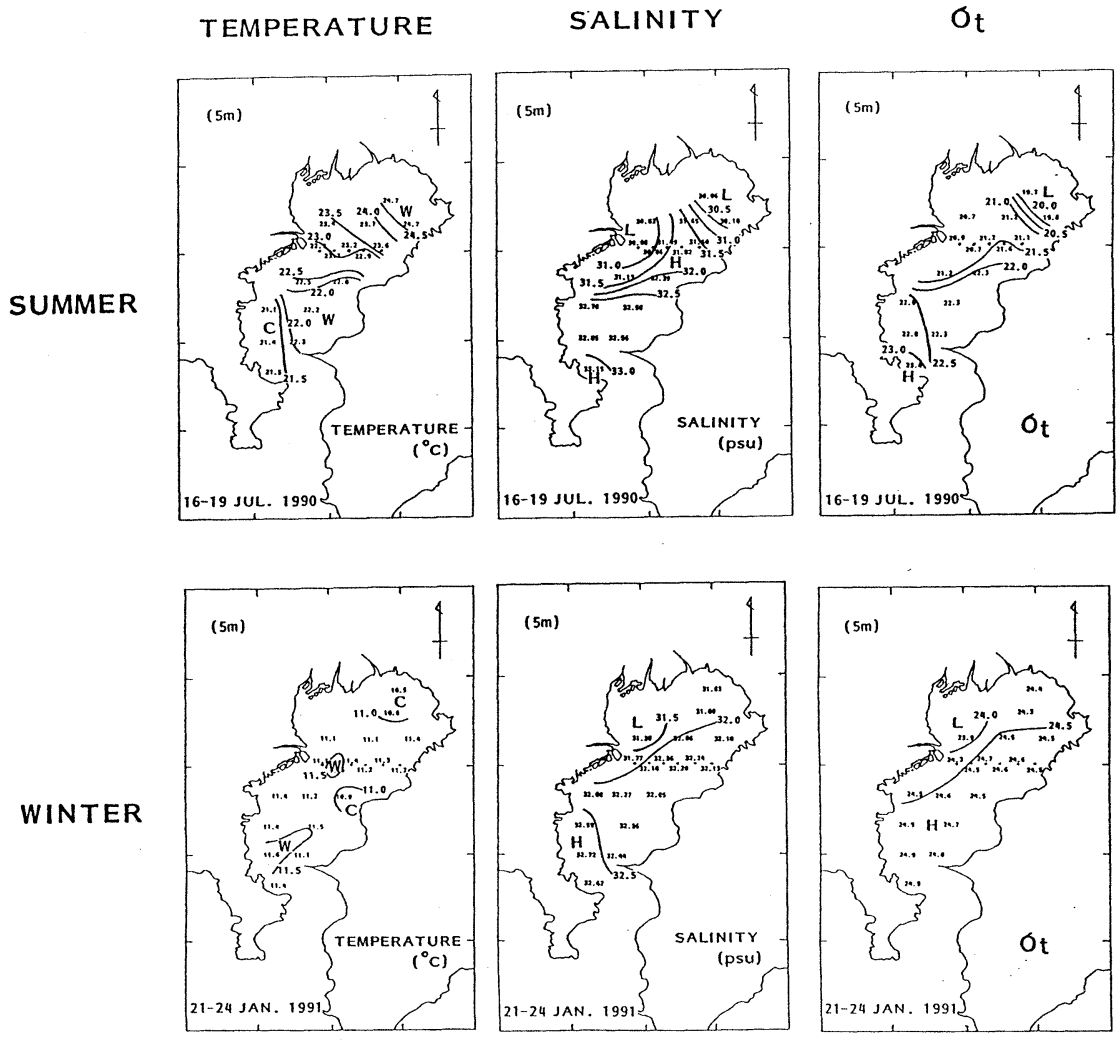

Fig. 5. Observed water temperature, salinity and density distributions in the upper layer in summer (upper) and in winter (lower).

Agency, 1991) are shown in Fig.5. The calculated distributions well reproduce the patterns of observed ones though the absolute values are a little different. The distribution patterns of water temperature, salinity and density in other layers (not shown) are also well reproduced by the numerical experiment.

The residual flows accompanied with calculated density distributions of Fig.4 are shown in Fig.6 (a) and (b). The clockwise residual circulation with the speed of about 10 cm s^{-1} is generated at the first layer in the central part of the bay in summer and the anticlockwise one with the speed of about 5 cm s^{-1} in winter. The residual circulation in the second layer is opposite to that in the first layer in summer but that is the same as the first layer in winter. There is no sufficient observational data on the distributions of residual flows of Tokyo Bay in summer and in winter. However, we may consider the residual flows in Fig.6 as reasonable ones because the distributions of water temperature and salinity are well reproduced as shown in Figs. (4) and (5).

The wind may affect the residual flow in Tokyo Bay but the wind is very variable with

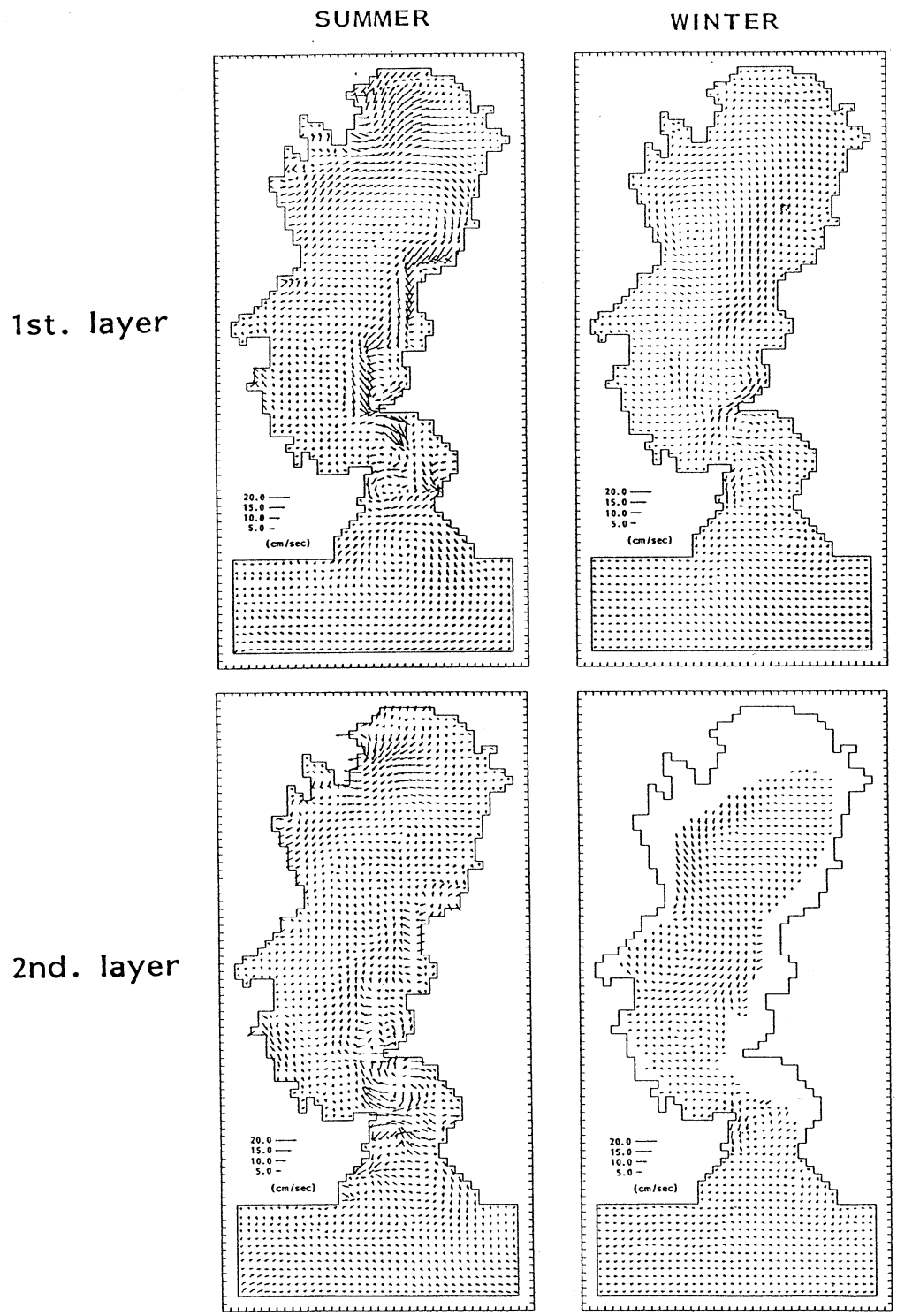

Fig. 6. Calculated residual flow in the upper (upper) and the middle (lower) layers in summer (left) and in winter (right).

the period of 3-4 days in summer and in winter. We carried out some numerical experiments with observed average wind in summer and in winter. However, we cannot reproduce the observed water temperature and salinity distributions under the constant wind blowing because the coastal upwelling is generated along the coast of Tokyo Bay by the northerly constant wind or southerly constant wind as discussed by MATSUYAMA *et al.* (1990). In the real field, the coastal upwelling phenomena are highly transient and are not steady state. We consider the time scale of 10-20 days in relation to the sedimentation process of particles in Tokyo Bay. Therefore, we take into account of only the tidal current and residual flow which consists of tide-induced residual current and density-driven current as the basic flow field in this numerical experiment of sedimentation in Tokyo Bay. The effect of wind to the movement of particles are included by the parameterization of wind into the wind wave in this numerical experiment which will be discussed later.

2.2 Sedimentation process

The Euler-Lagrange method is used to track the movement of particles in this numerical model. The position of particle X_{n+1} (x^{n+1}, y^{n+1}, z^{n+1}) at time n+1, which was X_n (x^n, y^n,z^n) at time n, can be calculated by the following equation:

$$X_{n+1}=X_n+v\Delta t+(\nabla v)v\Delta t^2+w_s\Delta t+R \quad (13)$$

where v denotes the calculated velocity vector including tidal current and residual flow; w_s, the sinking velocity of particle by the Stokes law ;

$$w_s = -\frac{g(\rho_p-\rho_w)}{18\mu r^2} \quad (14)$$

where g denotes the gravitational acceleration; ρ_p, density of particle; ρ_w, density of sea water; μ, ($=0.0115 cm^2 s^{-1}$), viscosity of sea water: r, diameter of particle. R is the dispersion due to the turbulence and is given by the following equation,

$$R_x \text{ and } R_y = \gamma\sqrt{2\Delta t D_h}, \qquad R_z = \gamma\sqrt{2\Delta t D_v} \quad (15)$$

where γ is the normal random number whose average is zero and whose standard deviation is 1.0; D_h ($=5 \times 10^5 cm^2 s^{-1}$) and D_v($=10 cm^2 s^{-1}$), the horizontal and vertical dispersion coefficient, respectively.

When particles reach the sea bottom, we judge whether it stops moving or removes by applying the critical tractive force theory (TSUBAKI, 1974):

$$F = \frac{\rho_w}{2} C_t U_b^2 \frac{\pi}{2} r^2 \quad (16)$$

$$R = \frac{\pi}{6} r^3 (\rho_p-\rho_w)\mu_s g \quad (17)$$

where F denotes the tractive force; R, the resistance force; C_t (= 0.4), drag coefficient of particle; μ_s (= 1.0), static friction coefficient of particle: U_b, the velocity just above the sea bed. We assume the velocity just above the sea bed is 0.2 times that of calculated velocity in the lowest layer of the numerical model and it is given by the following formula;

$$U_b = 0.2(U_t+U_r)+U_{wave} \quad (18)$$

where U_t denotes the calculated tidal velocity: U_r, calculated residual velocity and U_{wave} the water velocity due to wind wave and it is given by the following formula on the basis of small-amplitude wave theory;

$$U_{wave} = \frac{H_{wave} gT}{2L\cosh(2\pi H/L)} \quad (19)$$

where H denotes the water depth and H_{wave}, T and L wave height, wave period and wave length of dominant maximum wave in Tokyo Bay, respectively. The wave length depends on the water depth and the wave period and it is calculated as follows,

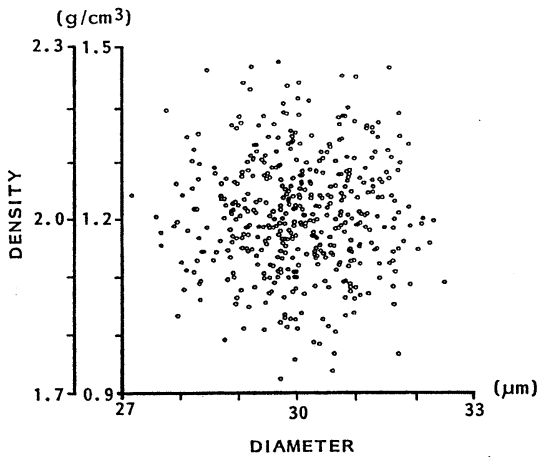

Fig. 7. Heavy and light groups of injected particles.

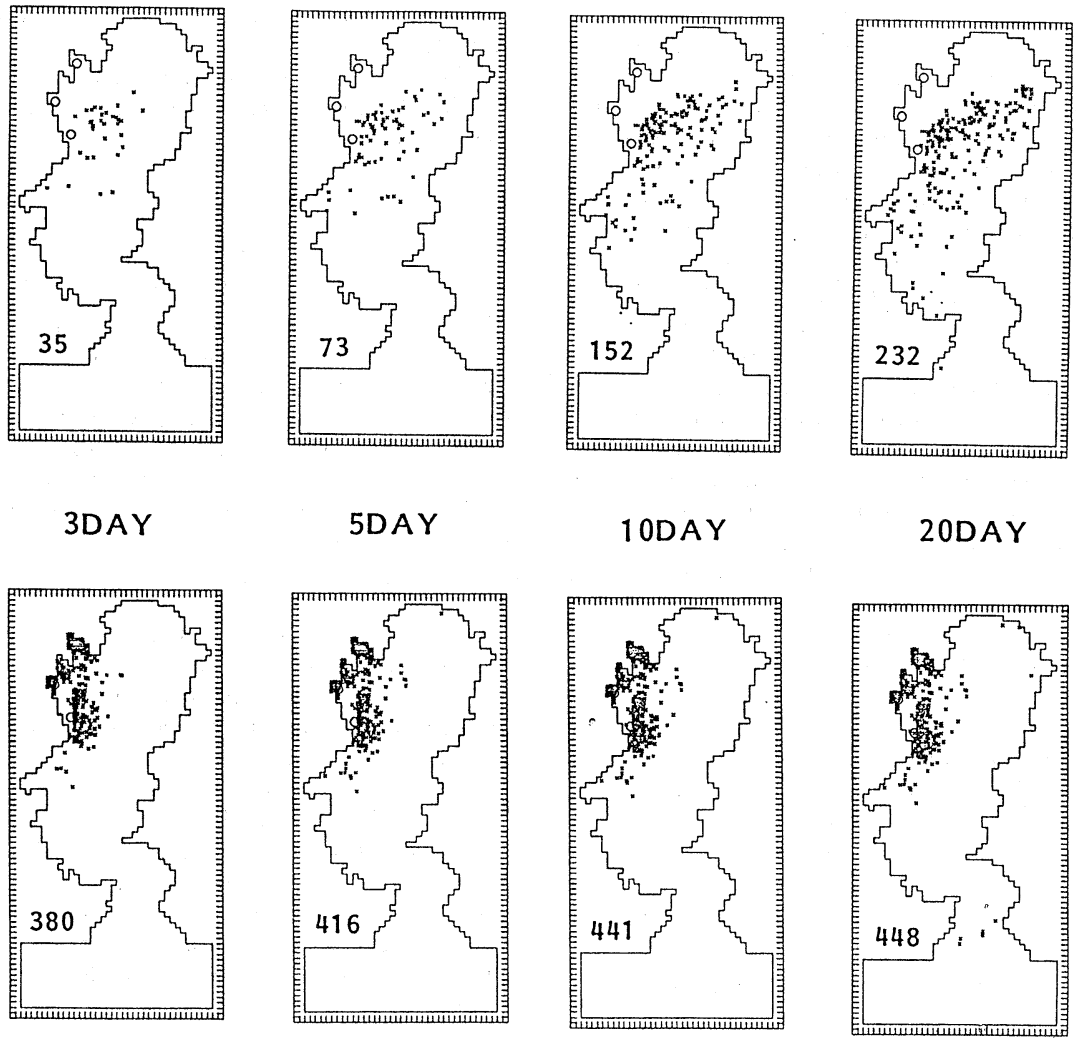

$$L = \frac{gT^2}{2\pi} \tanh \{2\pi (\frac{H}{gT^2})^{1/2} (1+(\frac{H}{gT^2})^{1/2}\} \quad (20)$$

The dominant wave height and wave period in Tokyo Bay were obtained by the field observation (Port Bureau of Tokyo Metropolitan, 1991). The used dominant maximum wave height and period in this numerical experiments are 80 cm and 3.0 sec, respectively and they are the same in summer and in winter. This is due to that the northerly wind is strong but the fetch is short in winter and the southerly wind is not so strong but the fetch is long in summer.

When R is larger than F, the particle stops moving and settles to the position where the particle reach the sea bottom and when F is larger than R, it removes from its position.

3. Results

Two groups of particles as shown in Fig.7 are injected from three river mouths which are

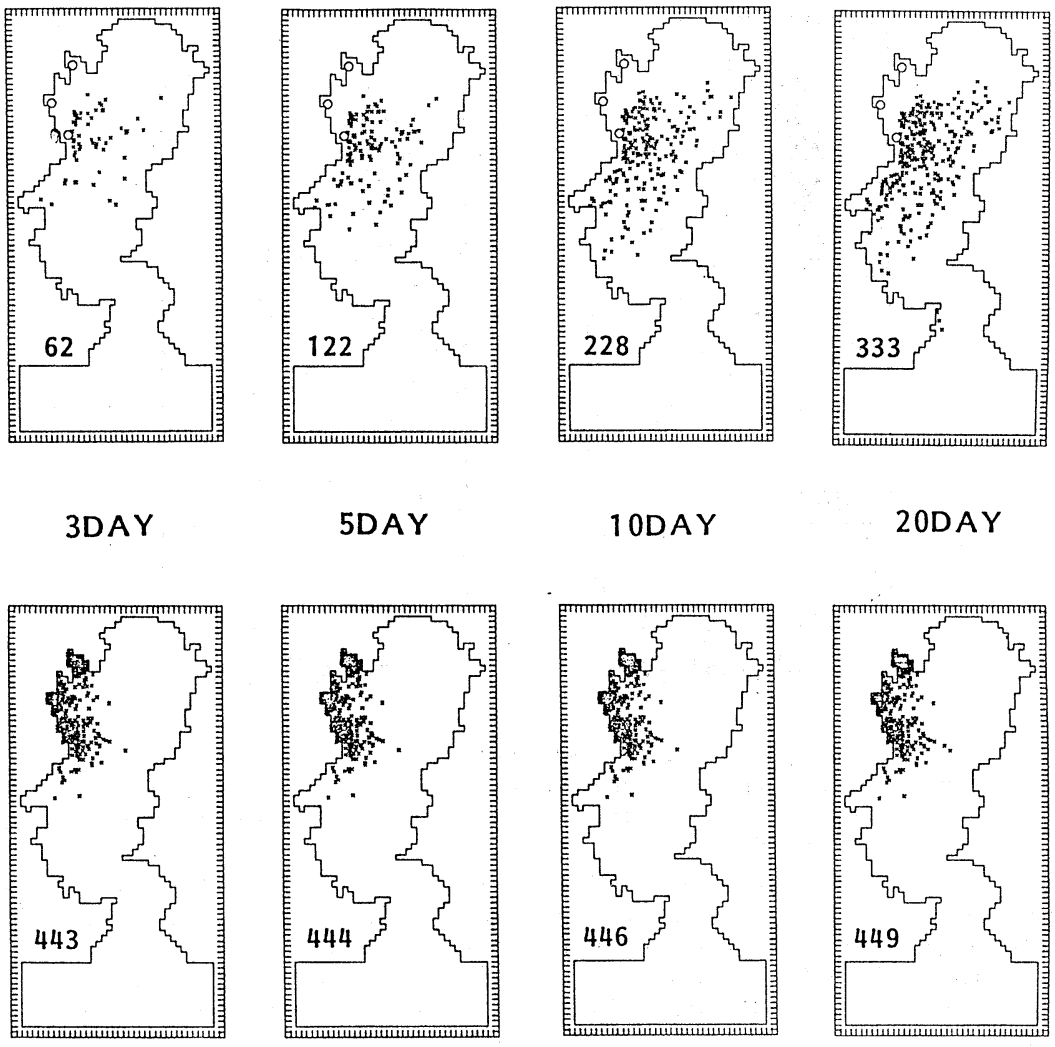

Fig. 8. Sedimentation patterns of light particles (upper) and heavy particles (lower) 3, 5, 10 and 20 days after the injection in summer (a) and in winter (b). Number means the number of settled particles.

shown in Fig.2. Heavy particles have the average diameter of 30 μm with the standard deviation of 1 μm and the average density of 2.0 g cm^{-3} with the standard deviation of 0.1 g cm^{-3} and light particles have the same average diameter and the average density of 1.2 g cm^{-3}. Such values are decided from the results of field observation in Tokyo Bay (R. ISHIWATARI, personal communication).

150 particles are injected from each river mouth and the total number of injected particles are 450. The results of numerical experiments are shown in Fig. 8 (a) and (b). Light particles settle in the central part of the bay while heavy particles settle near the river mouths in summer and in winter. Light particles can not settle near river mouth where the water depth is shallow and the current speed due to wind wave is large. On the oter hand, heavy particles can settle in the shallow part because the resistance

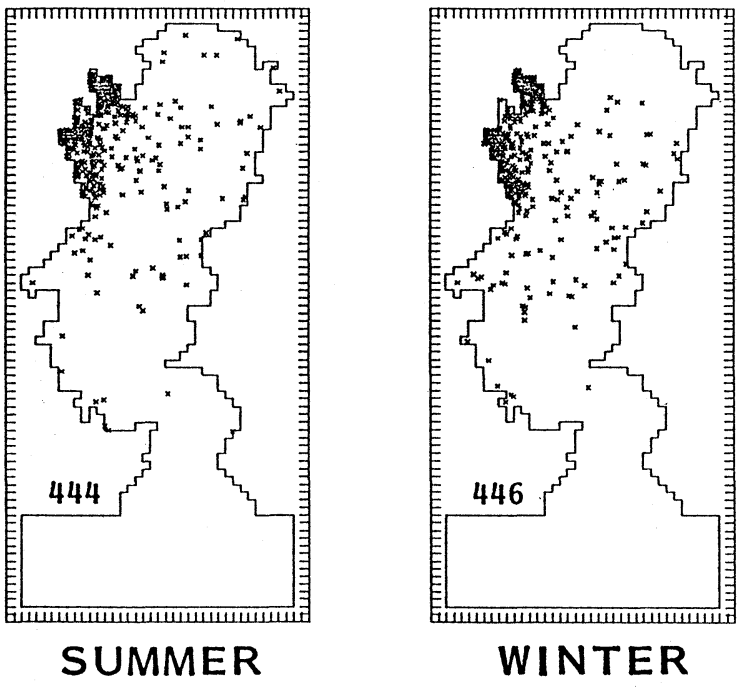

Fig. 9. Sedimentation patterns of light particles in the case of no wind wave 20 days after the injection in summer (left) and in winter (right). Number means the number of settled particles.

force R is large due to large particle density. The sedimentation pattern of light particles is simmilar to the circular shaped sedimentation pattern shown in Fig. 1 (b) and that of heavy particles to the fan shaped one shown in Fig. 1 (a).

The effect of wind wave is the largest in the difference of sedimentation patterns of light and heavy particles in Tokyo Bay because the velocities just above the sea bottom in Eq. (18) are $0.2 \times U_t \simeq 1.0$ cm s^{-1}, $0.2 \times U_r \simeq 0.4$–$1.0$ cm s^{-1} and $U_{wave} \simeq 2.0$ cm s^{-1} in the shallow part and $0.2 \times U_t \simeq 1.0$ cm s^{-1}, $0.2 \times U_r \simeq 0.4$-$1.0$ cm s^{-1} and $U_{wave} \simeq 0.02$ cm s^{-1} in the central part of the bay. The results of sedimentation pattern when the effect of wind wave is not included, are shown in Fig. 9. Light particles settle near the river mouth when the effect of wind wave is not included.

About half of light particles do not settle 20 days after the injection in summer while about 75 % settle in winter. The sinking velocity of particle shown in Eq. (14) and the resistance force shown in Eq. (17) are large and the tractive force is smaller in summer than in winter because the water density is smaller in summer. Such facts suggest that the settled number of particles is larger in summer than in winter while the calculated results show the oppositee results as shown in Fig. 8 (a) and (b). The difference of settled number of light particles 20 days after the injection between in summer and in winter is mainly due to the difference of speed of residual flow in summer and in winter because the speed of tidal current and that due to wind wave are the same in summer and in winter. The calculated speed of residual flow in the central part of the bay is 4–6 cm s^{-1} in summer and 2–3 cm s^{-1} in winter. The larger tractive force acts the particles in summmer than in winter and the settled number of light particles are smaller in summer than in winter.

4. Discussions

In these numerical experiments we change only the density of the particles without changing the diameter. We may obtain the same results if we change the diameter of particles without changing the density of particles because the sinking speed, tractive force and resistance force of particles depend on the density and diameter. Therefore we hope the chemical oceanographer to investigate the differences of average density or average diameter of particles to which riverine materials adhere in the near future.

In the real Tokyo Bay, particles may change its form from particulated state to dissolved state and vice verse. TAKEMATSU (1990) proposed another hypothesis that the fan shaped sedimentation is due to the inorganic particles and circular shaped one is due to the organic particles in Tokyo Bay. The rightness of his hypothesis has not been examined and we have to include such transformation of particles by the biochemical processes in the numerical model in the near future.

Acknowledgments

The authors express their sincere thanks to Dr. H. TAKEOKA of Ehime University, Prof. R. ISHIWATARI of Tokyo Metropolitan University and Dr. H. TAKADA of Tokyo University of Agriculture and Technology for their valuable discussions. A part of this study is defrayed by the Ministry of Education, Science and Culture, Japan.

References

Hydrographic Office of Maritime Safety Agency (1991): Observational results of water temperature and salinity in Tokyo Bay.

ISHIWATARI, R. (1988): Sedimentation process of land-derived organic matter in Tokyo Bay. Bulletin on Coastal Oceanography, **25**, 127–133 (in Japanese).

OONISHI, Y. (1978): Numerical simulation in the coastal sea. In "Science of Marine Enviroment" ed. by Y. Horible, Tokyo Univ. Press, Tokyo, 246–271 (in Japanese).

Port Bureau of Tokyo Metropolitan (1991): Wave Table in Tokyo Bay.

TAKEMATSU, N. (1988): Sedimentation pattern of riverine materials in the bay - concentric-fan-shaped sedimentation model. Bulletin on Coastal Oceanography, 25, 134–135 (in Japanese).

TSUBAKI, T. (1974): Hydraulics. Morikita Press, Tokyo, 210p. (in Japanese).

YANAGI, T., H. TSUKAMOTO, H. INOUE and T. OKAICHI (1983): Numerical simulation of drift cards dispersion. La mer, **21**, 218–224.

Y, T. and M. SHIMIZU (1991): Numerical experiment of sedimentation process in Tokyo Bay. Monthly Ocean, 23–4, 224–229 (in Japanese).

東京湾の堆積過程

柳　哲雄・清水　学

要旨：東京湾の表層堆積物の堆積パターンは，扇型パターンと円型パターンに大別される。前者はピレン・リン・銅などで，河口近傍に濃度最大域を有している。後者はアルキルベンゼン・炭素・カドニウムなどで，湾奥中央部に濃度最大域を有している。このような二つの堆積パターンが潮流・残渣流・密度分布・波浪による流れ・粒子の沈降速度を再現した3次元数値実験によりよく再現された。河川から流入した重い粒子は河口近傍ですみやかに堆積し，軽い粒子は河口近傍では堆積できず，流速の小さい湾奥中央部でのみ堆積する。したがって，重い粒子に吸着する諸物質は扇型パターンを，軽い粒子に吸着する諸物質は円型パターンを示すものと考えられる。